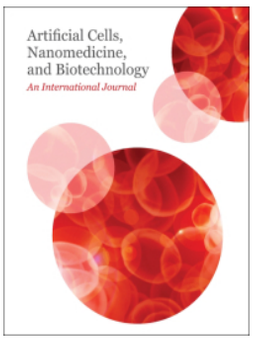

Taylor & Francis
Taylor & Francis Group

Artificial Cells, Nanomedicine, and Biotechnology
An International Journal

ISSN: (Print) (Online) Journal homepage: https://www.tandfonline.com/loi/ianb20

Myogenic commitment of human stem cells by myoblasts Co-culture: a static vs. a dynamic approach

Pasqualina Scala, J. Lovecchio, E.P Lamparelli, R. Vitolo, V. Giudice, E. Giordano, C. Selleri, L. Rehak, N. Maffulli & G. Della Porta

To cite this article: Pasqualina Scala, J. Lovecchio, E.P Lamparelli, R. Vitolo, V. Giudice, E. Giordano, C. Selleri, L. Rehak, N. Maffulli & G. Della Porta (2022) Myogenic commitment of human stem cells by myoblasts Co-culture: a static vs. a dynamic approach, Artificial Cells, Nanomedicine, and Biotechnology, 50:1, 49-58, DOI: 10.1080/21691401.2022.2039684

To link to this article: https://doi.org/10.1080/21691401.2022.2039684

ARTIFICIAL CELLS, NANOMEDICINE, AND BIOTECHNOLOGY
2022, VOL. 50, NO. 1, 49–58
https://doi.org/10.1080/21691401.2022.2039684

Myogenic commitment of human stem cells by myoblasts Co-culture: a static vs. a dynamic approach

Pasqualina Scala[a], J. Lovecchio[b,c], E.P Lamparelli[a]*, R. Vitolo[a], V. Giudice[a]*, E. Giordano[b,c,d], C. Selleri[a]*, L. Rehak[e], N. Maffulli[a]†[#] and G. Della Porta[a,f]

[a]Translational Medicine Laboratory, Department of Medicine, Surgery and Dentistry, University of Salerno, Via S. Allende, 84081 Baronissi, Salerno (SA), Italy; [b]Mol Cel Eng. Lab "S. Cavalcanti", Department of Electrical, Electronic and Information Engineering "Guglielmo Marconi" (DEI), University of Bologna, Via dell'Universitá 50, 47522 Cesena, Forlí-Cesena (FC), Italy; [c]Health Sciences and Technologies – Interdepartmental Center for Industrial Research (HST-ICIR), University of Bologna, Via Tolara di Sopra 41/E, 40064 Ozzano dell'Emilia, Bologna (BO), Italy; [d]Advanced Research Center on Electronic Systems (ARCES), University of Bologna, Via Vincenzo Toffano 2/2, 40125 Bologna (BO), Italy; [e]Athena Biomedical innovations, Viale Europa 139, Florence (FI), 50126, Italy; [f]Interdepartment Centre BIONAM, Università di Salerno, via Giovanni Paolo I, 84084 Fisciano, Salerno (SA), Italy

ABSTRACT

An *in-vitro* model of human bone marrow mesenchymal stem cells (*h*BM-MSCs) myogenic commitment by synergic effect of a differentiation media coupled with human primary skeletal myoblasts (*h*SkMs) co-culture was developed adopting both conventional static co-seeding and perfused culture systems. Static co-seeding provided a notable outcome in terms of gene expression with a significant increase of *Desmin* (141-fold) and *Myosin heavy chain II* (MYH2, 32-fold) at day 21, clearly detected also by semi-quantitative immunofluorescence. Under perfusion conditions, myogenic induction ability of *h*SkMs on *h*BM-MSCs was exerted by paracrine effect with an excellent gene overexpression and immunofluorescence detection of MYH2 protein; furthermore, due to the dynamic cell culture in separate wells, western blot data were acquired confirming a successful cell commitment at day 14. A significant increase of anti-inflammatory cytokine gene expression, including IL-10 and IL-4 (15-fold and 11-fold, respectively) at day 14, with respect to the pro-inflammatory cytokines IL-12A (7-fold at day 21) and IL-1β (1.4-fold at day 7) was also detected during dynamic culture, confirming the immunomodulatory activity of *h*BM-MSCs along with commitment events. The present study opens interesting perspectives on the use of dynamic culture based on perfusion as a versatile tool to study myogenic events and paracrine cross-talk compared to the simple co-seeding static culture.

ARTICLE HISTORY
Received 16 June 2021
Revised 10 December 2021
Accepted 1 February 2022

KEYWORDS
*h*BM-MSCs; human myoblasts; paracrine effect; myogenic commitment; perfusion bioreactor system

Introduction

Skeletal muscle tissue can heal spontaneously after an injury [1,2]. However, drug therapies with nonsteroidal anti-inflammatory drugs (NSAIDs), intramuscular corticosteroids, and operative management are often required; whereas, extended tissue damages need biological treatments, including cell therapy and tissue engineering [3].

In this field, *in vitro* models are extremely challenging and involve stem cells, such as bone marrow mesenchymal stem cells (BM-MSCs), and their ability to differentiate towards extremely diverse phenotypes under appropriate conditions [4–8]. Myogenic commitment of BM-MSCs involves key transcription factors and regulators as Myocyte Enhancer Factor-2 (MEF 2), Desmin [9,10], Myogenic Factor 5 (Myf 5), Myogenic Differentiation 1 (MyoD 1) [11], and Myogenin [12]. To promote myogenic commitment, culture medium can be supplemented with several growth factors, such as Hepatocyte growth factor (HGF) that has been described to promote myoblast proliferation and satellite cell activation [13,14], Insulin-like growth factor (IGF) that activate myoblast proliferation and differentiation [15], and Fibroblast growth factors (FGFs) that are involved in satellite cell proliferation and myoblast-to-myotube differentiation [16,17]. IGF, FGF, and HGF are usually added at a concentration of 10 ng/mL, while Epidermal growth factor (EGF) is used at 0.2 ng/mL [9,11,12]; however, the best mix and related concentration of growth factors for myogenic commitment are still unknown and under investigation. Myogenic commitment of BM-MSCs can also benefit by co-culture with skeletal muscle cells; however, seeding density ratios have not been well defined and standardised yet [9,10,12].

CONTACT Della Porta Giovanna gdellaporta@unisa.it Department of Medicine, Surgery and Dentistry, University of Salerno, Via S. Allende, Baronissi (SA), 84084, Italy
*Hematology and Transplant Center, University Hospital "San Giovanni di Dio e Ruggi D'Aragona", 84131 Salerno (SA), Italy.
[#]Centre for Sports and Exercise Medicine, Barts and The London School of Medicine and Dentistry, Queen Mary University of London, 275 Bancroft Road, London E1 4DG, England.

Supplemental data for this article is available online at https://doi.org/10.1080/21691401.2022.2039684.

During tissue regeneration, MSCs and immune cells strongly interact, favouring the healing process. Immune cell phenotype is largely influenced by MSCs thanks to their immune-modulatory effect [18]. MSCs reduce T-lymphocyte proliferation, causing their unresponsiveness by decreasing interferon-γ (IFN-γ) secretion [19] and preventing their activation [20], can favour T-lymphocyte and natural killer cell proliferation and viability, without affecting their anticancer cytotoxicity [21]. Macrophage polarisation seems to be influenced by MSCs *in-vitro*, especially by secretion of IL-10, an anti-inflammatory cytokine [22]. Particularly, BM-MSCs can suppress the expression of CD4 and CD8 by mononuclear cells and induce IL-6, IL-10, and TGF-β1 secretion [23], inhibit proliferation of B-lymphocytes and impair the secretion of immunoglobulins (IgM, IgG, IgA) [24]. Moreover, BM-MSCs have been reported to prevent the differentiation of monocytes into dendritic cells and to affect their antigen-presenting capacity [25].

Perfusion bioreactor systems have been also described to promote *in vitro* models. These culture systems have been used to improve the spatial uniformity of cardiac myocyte distribution on the 3D scaffolds and enhance the expression of cardiac-specific markers [26]. A perfusion system has been adopted to commit *h*BM-MSCs towards osteogenic and chondrogenic phenotype, showing that medium perfusion allowed a better distribution of soluble factors produced by cells as well as a more efficient mass transfer of nutrients [27–33]. On the other hand, more organised perfusion culture systems were adopted to understand paracrine effects between different cells in the so-called "*organ on chips*" systems that may involve microfluidic circuits for culture medium and different cell phenotypes to investigate molecular communication and/or cell interaction [34,35].

Considering all the described concepts, the present work aimed to investigate the myogenic commitment of *h*BM-MSCs, adopting a growth factor (bFGF) supplemented medium and a co-culture with human primary skeletal myoblasts (*h*SkMs) both in static and perfused conditions. Cells were co-seeded in the same well in static culture, whereas *h*SkMs and *h*BM-MSCs were seeded in separated wells by adopting the perfused bioreactor system culture. *h*BM-MSCs commitment was defined based on the expression of genes associated with myogenic phenotype, i.e. *Pax 3*, *MyoD 1*, *Myf 5*, *Myf 6*, *Desmin* and *Myosin heavy Chain II* (*MYH2*), on Desmin and MYH2 protein expression levels by semi-quantitative immunofluorescence (qIF) and by western blotting in dynamic co-culture conditions. Our study promoted the perfused co-culture system as a more versatile *in vitro* model to study myogenic differentiation events and cell cross-talk.

Materials and methods

hBM-MSC isolation and harvesting

*h*BM-MSCs were obtained from two healthy donors after informed written consent in accordance with the Declaration of Helsinki and protocol approved by Our Institutional Review Board (Ethics Committee "Campania Sud", Brusciano, Naples, Italy; prot./SCCE n. 24988). Protocols and data related to *h*BM-MSC characterisation by flow cytometry are reported in the Supplementary Materials section [36].

Cell culture

All cells were incubated at 37 °C in an atmosphere of 5% CO_2 and 95% relative humidity up to 21 days. *h*BM-MSCs at passage 2 were seeded at a density of 4,000 cells/cm^2 in a 12-well plate in a medium containing α-MEM supplemented with 1% Glutagro™ (Corning, Manassas, VA, United States), 10% FBS (Gibco™, Waltham, Massachusetts, United States), 100 nM dexamethasone (Sigma-Aldrich), 100 μM Ascorbic Acid (Sigma-Aldrich, Milan, Italy), and 1% Penicillin/Streptomycin (Corning).

hBM-MSCs-hSkMs static co-culture

*h*BM-MSCs were co-seeded with *h*SkMs (Gibco™) at a density of 4,000 cells/cm^2 at different ratios with a corresponding medium ratio of α-MEM supplemented with 1% Glutagro™ (Cornings), 10% FBS (Gibco™) and DMEM low glucose (Gibco™); medium also contains: 100 nM Dexamethasone (Sigma-Aldrich) always supplemented with 100 μM Ascorbic Acid (Sigma-Aldrich), and 1% Penicillin/Streptomycin (Corning).

Perfused medium bioreactor co-culture

Cells were cultured in a perfusion bioreactor formed by a custom multi-well plate milled in polymethyl methacrylate (PMMA, Altuglas® CN 100 10000, Altuglas International, La Garenne-Colombes Cedex, FR), a biocompatible material for biomedical applications [37]. This plate has two holes for silicon tube (Tygon®, Charny, France) insertion that allows the creation of a circuit in which medium flow is provided by peristaltic pumps at a constant flow rate of 1.0 ml/min [38]. In this case, *h*BM-MSCs and *h*SkMs were seeded at a density of 4,000 cells/cm^2 in different wells always maintaining the ratios of 2:1 or 1:1. Medium ratios were adjusted accordingly, as described before.

Brightfield images

Brightfield images of *h*BM-MSC and *h*SkM cultures were captured using a LEICA DMIL LED microscope, at 10× magnification, and acquired by LEICA DFC425 C camera.

RNA isolation and gene expression profiling

mRNA expressions were analysed by Reverse Transcription quantitative polymerase chain reaction (RT-qPCR). Total RNA was extracted using RNeasy Micro Kit (Qiagen, Hilden, Germany). For each sample, 1 μg of total RNA was reverse transcribed using iScriptTM cDNA synthesis kit (Bio-Rad, Milan, Italy), and relative gene expression analysis was performed on a LightCycler® 480 Instrument (Roche, Basel, Switzerland), using SsoAdvanced™ Universal SYBR® Green Supermix (Bio-Rad, Hercules, California, United States). Data were normalised to glyceraldehyde-3-phosphate dehydrogenase (*GAPDH*) applying the geNorm method [39] with CFX Manager software ($M < 0.5$), and fold changes in gene expression were determined by $2^{-\Delta\Delta CP}$ method and presented as relative levels over day 0 = 1.

Immunofluorescence assay

Cells were fixed with 4% paraformaldehyde for 30 min at RT followed by permeabilization with 0.1% Triton X-100 for 5 min and blocked with horse serum solution for 1 h. Cells were stained for Desmin (1:100; Abcam, Cambridge, UK) and for MYH2 (1:50, Thermo Fisher Sci., Waltham, MA, USA), and were incubated overnight at 4 °C. Subsequently, cells were incubated for 1 h at RT with Alexa Fluor™ 488 goat anti-rabbit IgG (1:400; Thermo Fisher Sci.) and with VectaFluor™ anti-mouse IgG Dylight 594® kit (Vector Laboratories, Burlingame, CA, United States) antibodies, and cell nuclei were counterstained using 4′,6-diamidino-2-phenylindole (DAPI). All images were acquired by a fluorescence microscope with identical settings (Eclipse *Ti* Nikon Corporation, Tokyo, Japan). Signals intensity was quantified using Image J software (rel.1.52p National Institutes of Health, USA). Original images in RGB format were converted into a 16-bit (grey scale) format. Then, tagged areas were expressed as an average value of pixel intensity within a range from 0 (dark) to 255 (white). Data were normalised to the number of cells present in the whole field and reported as fold change relative to *h*BM-MSCs at day 0 [40].

Western blotting

*h*BM-MSCs were lysed in ice-cold RIPA lysis buffer (50 mM Tris-HCl, 150 mM NaCl, 0.5% Triton X-100, 0.5% deoxycholic acid, 10 mg/mL leupeptin, 2 mM phenylmethylsulfonyl fluoride and 10 mg/mL aprotinin). About 10 μg of proteins were separated on 10% SDS-PAGE at 90 V for 1 h and at 120 V for 1 h and transferred on a nitrocellulose membrane. 5% non-fat dried milk powder (Sigma-Aldrich) in Tris-buffered saline containing 0.1% Tween-20 (TBST) was used for blocking for 1 h at RT. Primary antibodies, Desmin (Abcam ab8592, rabbit, 1:3000) and MYH2 (Thermo Fisher Sci., #PA5-116876, rabbit, 1:3000) were incubated overnight at 4 °C. Horseradish peroxidase-conjugated donkey anti-rabbit IgG (BioRad, Milan, Italy) was used to immunodetect proteins with chemiluminescence (ECL) system (Amersham Pharmacia Biotech, Piscataway, NJ) and exposed to X-ray film (Santa Cruz Biotechnology, Dallas, Texas, USA). The optical density (OD) of bands was analysed by Photoshop software and expressed as a ratio relative to actin-β protein.

Statistical analysis

Statistical analysis was conducted using Prism software (v.6.0, GraphPad Software, LLC, San Diego, California, United States). Results are presented as mean ± standard deviation (SD). Statistical analysis was performed using one-way analysis of variance (ANOVA) with Tukey's multiple comparison test, for comparison vs. *h*BM-MSCs at day 0, selected as control. Two-way analysis of variance (ANOVA) with Tukey's multiple comparison test was also performed for comparison of data obtained in perfusion system culture vs. *h*BM-MSCs at day 0. *P* values $< .05$ were accepted as significant [41].

Results

hBM-MSC and hSkM characterisation

Mesenchymal phenotype was confirmed according to minimal criteria defined by the International Society of Cellular Therapy [42]. In particular, primary *h*BM-MSC were positive for mesenchymal markers, such as CD90, CD105, and CD73, while negative for CD34, CD14, CD45, and HLA-DR by flow cytometry analysis (see also Figure S1 in Supplementary materials).

*h*SkMs showed their typical stretched shape, as observed by optical microscope images (see Figure 1a). q-IF analysis showed the two myogenic proteins, Desmin and MYH2. Desmin was better expressed in the first seven days of culture (41.7-fold), while MYH2 displayed an increasing trend up to day 21 (0.30-fold, $p \leq .0001$). (Figure 1b,c). Concerning gene expression, *Pax 3*, *MyoD 1*, *Myf 5*, *Myf 6*, *Desmin,* and *MYH2* were constitutively expressed in *h*SkMs, with *Pax 3* expressed earlier in the myogenesis process [43] (Figure 2).

Myogenic commitment strategies of hBM-MSCs

bFGF at a concentration of 10 ng/mL is largely recommended in literature as a supplement in the myogenic medium; however, when *h*BM-MSCs were cultured in static conditions within this environment, they exhibited poor changes in myogenic gene expression (Figure 2). Indeed, *Pax3* reached the maximum expression after 7 days of culture (34-fold), and *MyoD 1*, *Myf 5* and *Myf 6* sequentially picked the maximum of 30-fold, 23.6-fold, and 16.7-fold at day 7, respectively; then, these gene expressions were reduced. *Desmin* and *MYH2* genes were not up-regulated throughout the whole culture time.

On the contrary, when *h*BM-MSCs were co-seeded with *h*SkMs at a ratio of 2:1, an excellent myogenic gene expression outcome was observed (Figure 2): *MyoD 1* expression was remarkable with the maximum statistically significant expression at day 14 with 3400-fold, while *Myf 5* and *Myf 6* reached the highest expression at day 7, with 2000-fold and 590-fold, respectively. *Desmin* was up-regulated at day 7 of 88-fold and at day 21 of 141-fold ($p \leq .001$). *MYH2* increased to 13-fold on day 14 and up to 32-fold ($p \leq .0001$) on day 21. *h*SkM gene expression, normalised on *h*BM-MSCs at day 0, were added to Figure 2, as a positive control. From morphological analysis, *h*BM-MSC-*h*SkMs co-seeded showed a progressive elongated shape with an even more accurate orientation along the paralleled line (brightfield images in Figure 3a). This behaviour was particularly evident in zoomed areas at 150% inserted in each image of Figure 3a. IF images showed the presence of Desmin, as confirmed by q-IF with 1.5-fold ($p \leq .001$) at day 7, and an increasing trend of MYH2 protein secretion, 1.1-fold ($p \leq .001$) at day 21. From IF images, *h*SkMs nuclei clearly grouped appeared at day 14, forming the typically polynuclear syncytia, that can distinguish them from *h*BM-MSCs (Figure 3b). *h*BM-MSCs were significantly stained in green, the fluorochrome associated with MYH2. Poor *h*BM-MSC viability was observed when a 1:1 cell ratio was adopted (data not shown).

To study the immunomodulatory activity of *h*BM-MSCs along with myogenic commitment events, cytokine expressions were

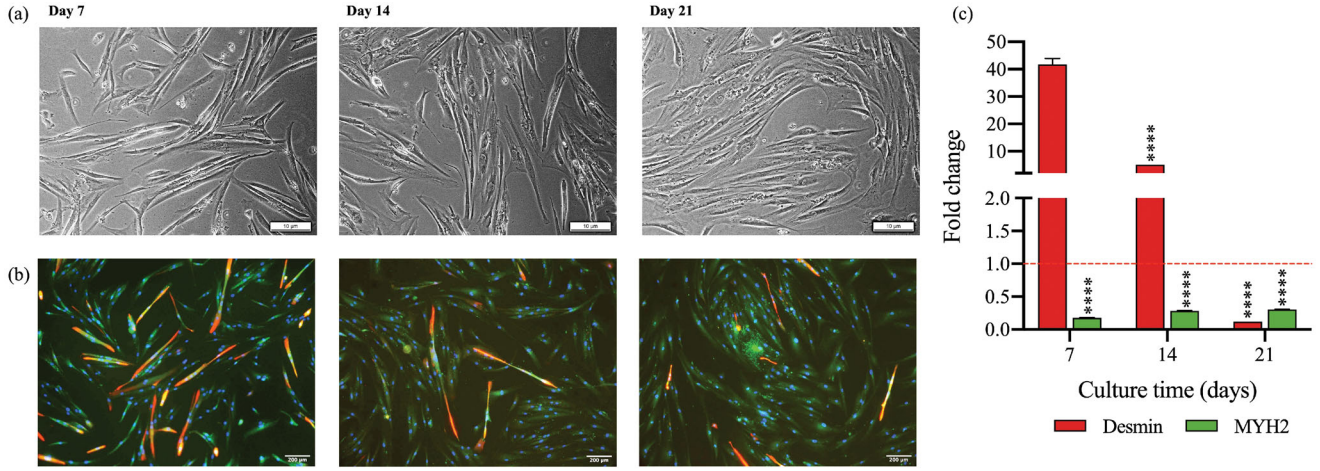

Figure 1. Brightfield images and immunofluorescence assay of *h*SkMs. Brightfield images of *h*SkMs, seeded at a density of 120.000 cells/cm^2, at days 7, 14 and 21 of culture. All images were captured using 10× magnification; scale bar: 10 μm (a). IF assay at days 7, 14 and 21 of culture was performed by staining Desmin in red and MYH2 in green. All images were captured using 10× magnification, scale bar: 200μm (b). Semi-quantitative IF of Desmin and MYH2 protein signals is shown as mean ± SD, and two-way ANOVA performed between time points, $n = 3$, $^{*}p < .05$, $^{**}p < .01$, $^{***}p < .001$ and $^{****}p < .0001$ (c).

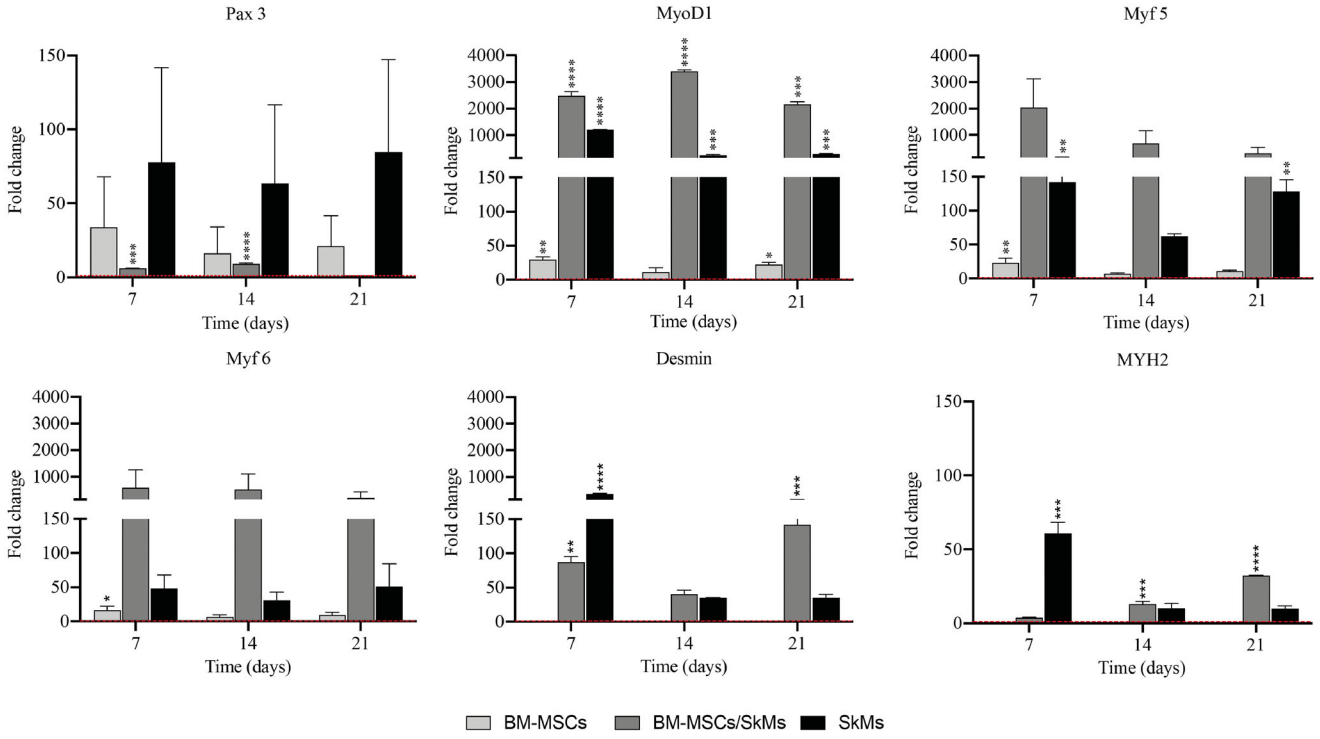

Figure 2. Gene expression profiling for myogenic markers by quantitative RT-PCR obtained from *h*BM-MSCs and *h*SkMs co-seeding culture in static condition with myogenic medium (10 ng/mL of bFGF). *h*BM-MSCs were co-seeded with *h*SkMs in ratio 2:1; *h*BM-MSCs and *h*SkMs were added, as controls. mRNA levels of myogenic markers: *Pax 3, MyoD 1, Myf 5, Myf 6, Desmin* and *MYH2* were assayed by qRT-PCR at days 7, 14 and 21 of culture. The relative quantification of each mRNA gene expression normalised to endogenous GAPDH (internal control) was calculated using the $2^{-\Delta\Delta Ct}$ method and presented as fold change over *h*BM-MSCs at day 0, selected as a control. All data were analysed by one-way ANOVA, $n = 3$; $^{*}p < .05$, $^{**}p < .01$, $^{***}p < .001$ and $^{****}p < .0001$.

investigated (Figure 4). *h*BM-MSCs culture with bFGF supplemented medium upregulated *IL-12A* at 67.5-fold at day 7; *IL-1β* reached 4-fold at day 7, then those expressions were significantly reduced along the further culture time. Among anti-inflammatory cytokines, *IL-4* and *IL-10* were the most overexpressed with the maximum fold reached by *IL-4* of 44-fold and by *IL-10* of 27-fold, both statistically significant, at day 7 (Figure 4). In static co-seeding culture, *TNF-α* was the highest up-regulated pro-inflammatory cytokine, followed by *IL-1β* and *IL-12A*. The maximum peak at day 14 was for *TNF-α* (8-fold), *IL-1β*, (6-fold) and for *IL-12A* (4-fold). All expressions returned close to baseline levels at day 21 (Figure 4).

Most significantly cytokines expressed by *h*SkMs were *TNF-α* (9-fold) at day 7; *IL-1β* (205-fold), *IL*-10 (90-fold) overexpressed and *IL-4* (117-fold) were overexpressed at day 14. TGF-β1 and TGF-β2 expression increased of 3.4-fold and 1.2-fold at day 7, respectively, showing a different behaviour with respect to co-seeding culture (Figure 4).

The described data indicated that *h*BM-MSCs showed poor myogenic gene expression when cultured with bFGF

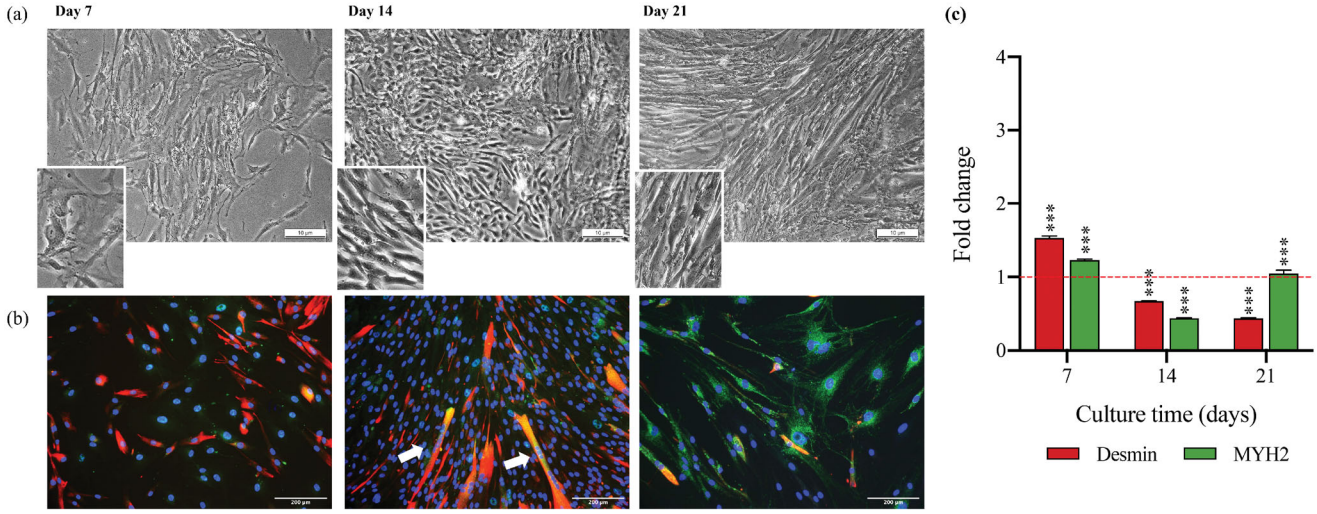

Figure 3. Brightfield and immunofluorescence (IF) images of *h*BM-MSCs and *h*SkMs co-seeded with ratio 2:1 in static condition with myogenic medium (10 ng/mL of bFGF). Brightfield images at days 7, 14 and 21 were captured using 10× magnification; scale bar: 10 μm; a zoomed area at 150% was added to better show the morphology of the cells and their elongation (a). IF assay was performed at the same time points by staining Desmin in red and MYH2 in green. All images were captured using 20× magnification, scale bar: 200 μm. Several *h*SkMs multinucleate cells are evident (see arrowheads); the Desmin protein (see red staining) is mainly localised nearby. MYH2 (see green staining) was a more abundantly distributed overall cell population. From the images, it was also clear the cells alignment and their longitudinal elongation (b). Semi-quantitative IF of Desmin and MYH2 protein signals is shown as mean ± SD, and two-way ANOVA performed between time points, $n = 3$, $^{*}p < .05$, $^{**}p < .01$, $^{***}p < .001$ and $^{****}p < .0001$ (c).

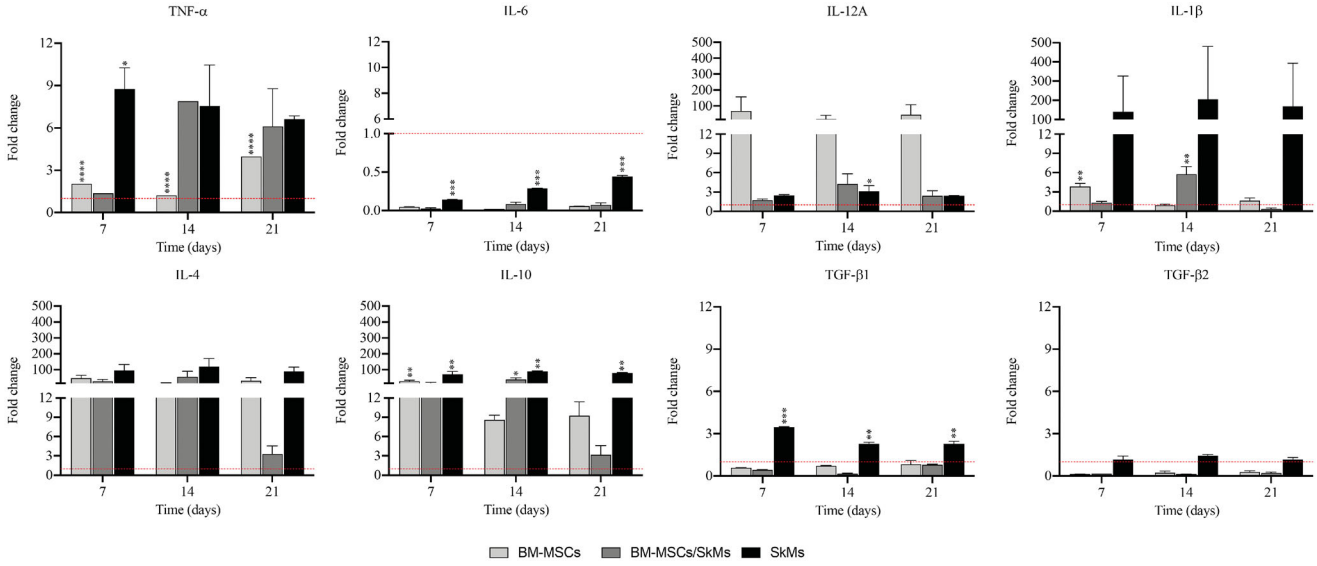

Figure 4. Gene expression profiling for pro- and anti-inflammatory cytokines by quantitative RT-PCR obtained from *h*BM-MSCs and *h*SkMs co-seeding culture in static condition with myogenic medium (10 ng/mL of bFGF). *h*BM-MSCs were co-seeded with *h*SkMs in ratio 2:1; *h*BM-MSCs under bFGF medium and *h*SkMs were added as controls. The mRNA levels of pro-inflammatory cytokines (*TNF-α, IL-6, IL-12A* and *IL-1β*) and anti-inflammatory cytokines (*IL-10, IL-4, TGF-β1* and *TGF-β2*) were assayed by qRT-PCR at days 7, 14 and 21 of culture. The relative quantification of each mRNA gene expression normalised to endogenous GAPDH (internal control) was calculated using the $2^{-\Delta\Delta Ct}$ method and presented as fold change over *h*BM-MSCs at day 0, chosen as control. All data were analysed by one-way ANOVA, $n = 3$; $^{*}p < .05$, $^{**}p < .01$, $^{***}p < .001$ and $^{****}p < .0001$.

supplemented medium; whereas static *h*BM-MSCs and *h*SkMs (ratio 2:1) co-seeding induced an excellent expression of myogenic markers.

Dynamic culture system

When *h*BM-MSCs were cultured under bFGF supplemented medium in a dynamic environment, a total absence of myogenic gene expression was observed (despite the control gene *GADPH* being monitored correctly); IF observation confirmed the total absence of myogenic proteins (data not shown).

When, *h*BM-MSC and *h*SkM dynamic co-culture was tested, the two different cell populations were spatially separated, since they were seeded in different wells, even if the same culture medium was flowing along with the whole culture (Figure 5). In this dynamic arrangement, cell ratios explored were of 2:1 and 1:1 (*h*BM-MSCs:*h*SkMs); a poor cell survival was observed for the 1:1 ratio (data not shown); therefore, all following data are related to culture achieved adopting the 2:1 ratio.

In such cases, *h*BM-MSCs showed an excellent up-regulation of myogenic genes (Figure 6a). *Pax 3* was up-regulated 11-fold at day 7; myogenic regulation factors (MRFs), at day 7 showed

the highest up-regulation of 9-fold for *MyoD 1*, 38-fold for *Myf 5* and 37-fold for *Myf 6*. *Desmin* showed a constant up-regulation throughout the dynamic culture, with 10-fold at day 7, 16-fold at day 14 and 9.5-fold at day 21. *MYH2* increase was 4.4-fold on day 7.

Cytokine expression by *h*BM-MSCs, normalised over day 0, was also investigated (Figure 6b).Overall anti-inflammatory cytokine upregulation with respect to pro-inflammatory ones was observed, as monitored in static co-seeding culture. More in detail, *IL-12A* showed an increasing trend with 2-fold, 5-fold, and 7-fold at the investigated time points, while *IL-1β* expression was almost constant along the culture (1-fold change). Other pro-inflammatory cytokines, such as *IL-6*, *TNF-α* and *IFN-γ*, were not detected. Among anti-inflammatory cytokines, *IL-10* and *IL-4* were the most upregulated: i.e. *IL-10* reached the maximum spike of expression at day 21 with 19.2-fold and *IL-4* at day 14 with 11-fold. TGF-β expression was quite low, except for *TGF-β1* at day 7 (4-fold).

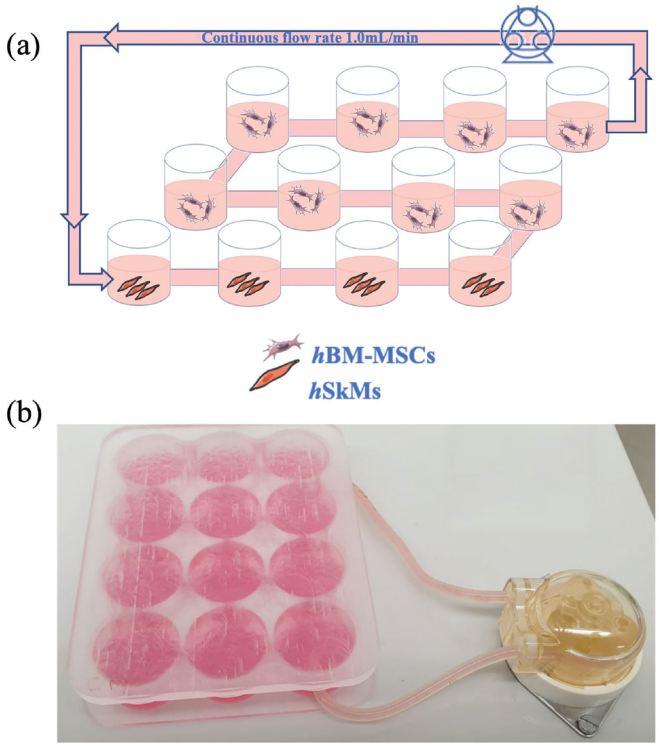

Figure 5. Schematic representation and image of perfused bioreactor system used for the dynamic co-culture of *h*BM-MSCs with *h*SkMs (2:1). *h*BM-MSCs were cultured in myogenic medium supplemented with 10 ng/mL of bFGF with perfused *h*SkMs medium up to 21 days. The number of the well were loaded to maintain the same cell ratio of 2:1, respectively, as studied in static culture. Each well has an internal diameter of 2 cm; the mean flow rate was 1 mL/min.

IF staining performed on *h*BM-MSCs cultured within the perfusion system showed a significant signal for Desmin (stained in red) at earlier time points and a significantly more intense signal for MYH2 (stained in green) especially at day 21 (Figure 7b); q-IF confirmed a statistically significant increase of 2.4-fold ($p \leq .001$) at day 7 and 2.9-fold ($p \leq .01$) for Desmin and of 2.25-fold ($p \leq .001$) at day 7and 2.5-fold ($p \leq .01$) at day 21 for MYH2 (Figure 7c). Furthermore, *h*BM-MSCs showed an extremely ordinate alignment with a clearly elongate shape. When similar IF staining was performed on *h*BM-MSCs supplemented only with bFGF medium, neither Desmin nor MYH2 signals were observed (Figure 7a). In dynamic culture, *h*BM-MSCs and *h*SkMs were seeded independently, Desmin and MYH2 production was monitored also by western blot assay (Figure 8). Both proteins showed similar expression trends with a significant increase at day 7 and the maximum expression at day 14.

The described data suggested that *h*BM-MSC co-culture in perfusion undergoes a successful myogenic commitment with significant upregulation of all gene markers and anti-inflammatory cytokines with Desmin and MYH2 protein production.

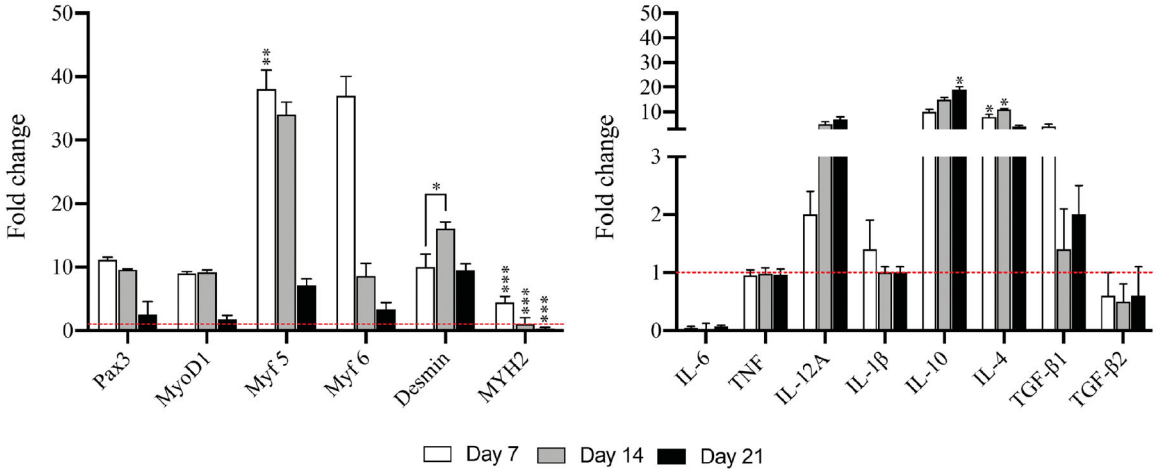

Figure 6. Gene expression profiling of myogenic markers and cytokines expressed by *h*BM-MSCs within perfusion bioreactor culture. mRNA levels of myogenic markers (*Pax 3, MyoD 1, Myf 5, Myf 6, Desmin* and *MYH2*), pro-inflammatory cytokines (*IL-6, IL-12A, IL-1β*) and anti-inflammatory cytokines (*IL-10, IL-4, TGF-β1, TGF-β2*) were monitored. Relative quantification of each mRNA gene expression normalised to endogenous GAPDH (internal control) was calculated using the $2^{-\Delta\Delta Ct}$ method and presented as fold change over *h*BM-MSCs and *h*SkMs collected at day 0 = 1. Two-way analysis of variance (ANOVA) with Tukey's multiple comparison test was performed for comparison of data obtained at Day 0 in perfusion system culture. $n = 3$. $^{*}p < .05$, $^{**}p < .01$, $^{***}p < .001$.

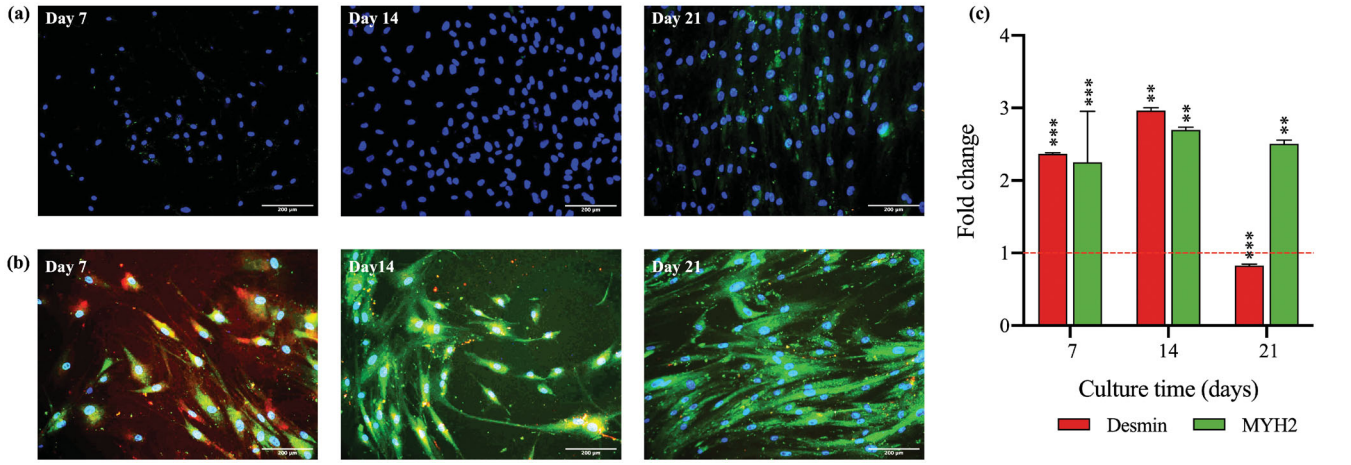

Figure 7. Immunofluorescence (IF) images of *h*BM-MSCs with myogenic medium and under co-culture within perfusion bioreactor. IF assay at days 7, 14 and 21 of culture was performed by staining Desmin in red and MYH2 in green. The images illustrated *h*BM-MSCs cultured in myogenic medium (a) and *h*BM-MSCs cultured in co-culture thanks to the perfusion system, in such case cells orientation and elongation and the presence of the myogenic protein are evident (b). All images were captured using 20× magnification. Scale bar: 200 μm. Semi-quantitative IF of Desmin and MYH2 protein signals from *h*BM-MSCs is shown as mean ± SD, and two-way ANOVA performed between time points, $n = 3$, $^{*}p < .05$, $^{**}p < .01$, $^{***}p < .001$ and $^{****}p < .0001$ (c).

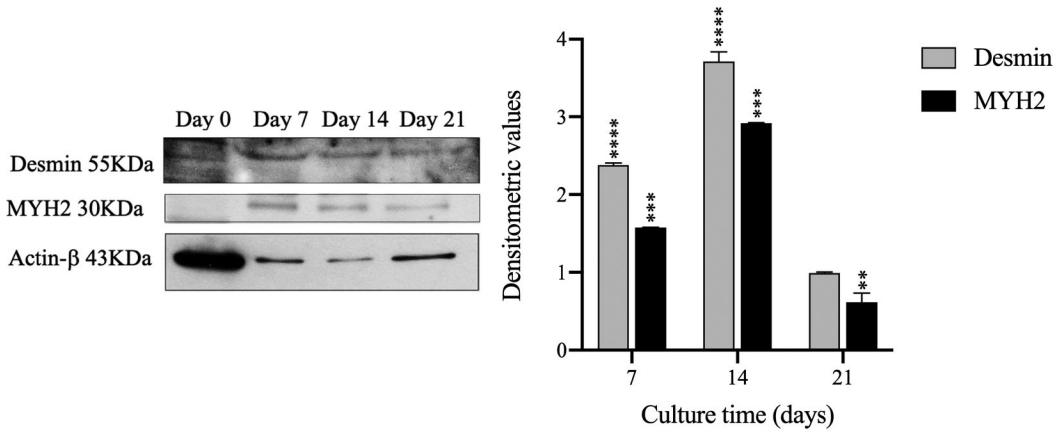

Figure 8. Western blot assay for Desmin and MYH2 proteins. Desmin and MYH2 proteins were detected through western blot analysis in *h*BM-MSCs cultured in perfusion system on days 7, 14 and 21. Data were normalised against actin-β and reported as mean value ± SD ($n = 3$). The blotting outcomes confirmed the presence of both proteins suggesting a clear *h*BM-MSCs commitment versus the myogenic phenotype. Two-way ANOVA was performed between time points, $n = 3$, $^{**}p < .01$, $^{***}p < .001$ and $^{****}p < .0001$.

Discussion

bFGF supplemented medium showed low myogenic potential, whereas co-seeding *h*BM-MSCs with *hSkMs* promoted myogenic commitment events when a 2:1 ratio was adopted.Cell co-culture system was achieved by conventional static culture and by using a perfusion bioreactor to promote cell cross-talk by paracrine *via*. In both cases, the whole myogenic gene expression was progressively upregulated, probably due to a complex biochemical cell-to-cell cross-talk [44,45]. The expected commitment was checked by evaluating all MRF gene expressions, that act in a concerted manner and with a specific spatio-temporal expression during myogenesis. Indeed, the early factors (*MyoD 1* and *Myf 5*) are involved in the commitment and proliferation of myogenic directed cells, and late factors (*Myf 6*) regulate terminal differentiation of committed cells, even if they can functionally overlap [46]. The *h*SkMs constitutively and constantly expressed these genes along the culture therefore when the same genes were upregulated in *h*BM-MSCs, an effective myogenic commitment of stem cells was assumed.

The co-seeding system in a static culture environment promoted myogenic events but has poor versatility, and the recovery of single-cell population for proper investigation is not even possible. On the contrary, co-culture adopting the perfusion system ensured successful outcomes and allowed cell collection independently. Additionally, it can be considered an excellent system to investigate *in vitro* the myogenic commitment by paracrine *via*. Indeed, in such a case, gene expression seemed to follow the same progression of commitment events previously observed in co-seeding experiments, suggesting that a paracrine effect could induce cell commitment versus a specific phenotype, probably thanks to complex cross-talk even in absence of direct cell-to-cell contact. In perfused systems, *h*BM-MSCs expressed and upregulated the same genes, such as *Pax 3* and the whole MRFs. *Pax 3* was overexpressed at day 7 (11.1-fold) and then its expression decreased; the same behaviour was observed for *Myf 5* and *Myf 6* that were significantly upregulated at day 7 of culture (38-fold, $p < .01$; 37-fold, respectively), followed by a decreasing trend observed at day 21. *Desmin* expression also significantly increased at day 14 (16-fold, $p < .05$),

whereas *MYH2* started to be overexpressed significantly (4-fold, $p < .001$) at day 7. Despite an apparently not largely overexpression of *Desmin* and *MYH2* genes, with respect to all MRFs, when protein characterisation was performed through western blot assay, a clear presence of both Desmin and MYH2 protein bands was monitored confirming the proper myogenic commitment. Both proteins follow the same expression trend with the maximum peak at day 14, with Desmin more abundant than MYH2, because t Desmin constitutes intermediate filaments, and its expression is temporarily earlier than MYH2, that takes part of the contractile system.

The biochemistry behind how *h*BM-MSCs acquire myogenic phenotype is complex and many aspects remain still unclear. The unique commitment of *h*BM-MSCs towards myogenic phenotype occurs when *Pax 3* signalling activates [46,47]; indeed, *Pax 3* seems to act independently from Notch pathway, as Hes 1 and Hes 5 are not upregulated. Moreover, *Pax 3* is the first transcription factor of myogenesis that regulates MRFs expression and blocks other potential mesenchymal differentiation events, such as adipogenesis, osteogenesis and chondrogenesis. In our study, in all experimental conditions, *Pax 3* showed a good expression, reducing over culture time in favour of MRFs expression; thus, we could assume that *h*BM-MSCs were successfully committed towards myogenic phenotype. Some authors also described that the canonical Wnt pathway leads to β-catenin stabilisation, that, once in the nucleus, can induce the expression of target genes, such as MRF expression [47]. However, further investigations are required to better characterise the whole Wnt pathway. In this sense, our *in vitro* model may be also useful for these studies. In almost all experiments, best gene overexpression and protein production were monitored at day 14 of culture; this can be probably due to the fact that long-term culture can affect biological activity of MSCs, as largely reported in literature [48]

Since *h*BM-MSCs show an immunomodulatory capacity, a broad range of cytokines has been investigated to understand which are expressed during the commitment process, considering that all of them play a pivotal role during myogenesis. For example, the role of TNF-α during myogenesis is still controversial and some authors reported TNF-α as an autocrine factor as it is constitutively expressed by myoblasts and largely released under differentiation stimuli [49,50]. On the other hand, TNF-α mostly contributes to myoblast proliferation by accelerating cell cycle progression [51,52]. In our study, *h*SkMs showed a low expression of *TNF-α* and its expression was not detected in perfusion system culture even if it increased 8-fold in co-seeded static culture (Figure 4). IL-1 is involved in myogenesis and seems to favour myoblast mitosis, enhancing muscle protein synthesis [53]. However, conflicting data are reported on IL-1 role because prolonged exposure can allow a reduction in myotube width and actin levels [54]. Detected expression of *IL-1β* was very high in *h*SkMs up to 205-fold, while *h*BM-MSCs under bFGF medium expressed it only 4-fold ($p < .01$) at 7 days; in co-seeded static culture, the expression of this cytokine increased at 6-fold ($p < .01$) at 14 days, and it was overexpressed 1-fold at day 7 in the dynamic system.

IL-10 is an anti-inflammatory cytokine mostly involved in skeletal muscle regeneration, favouring newly regenerating myofibers [55]. The highest expression value of *IL-10* was detected in *h*SkMs (89.9-fold $p < .01$) at day 14, followed by co-seeding static culture (38-fold $p < .05$), at the same time point. In the perfusion system, the expression of *IL-10* was lower than static co-seeding culture, but one of the most upregulated (19.2-fold, $p < .05$) at day 21. The same trend was detected for *IL-4*. This cytokine promotes muscle differentiation [56,57]. In *h*BM-MSCs static co-seeding, the expression of *IL-4* is high up to 55-fold and, in the perfusion system, *IL-4* is one of the most upregulated of 11-fold ($p < .05$) at same day 14. TGFβ family members do not exceed 4-fold, both in static and in perfusion system.

In static co-seeding culture, the overall expression of pro-inflammatory cytokines was balanced by the high expression of anti-inflammatory ones, such as *IL-10* (38-fold, $p < .05$) and *IL-4* (55-fold). In the perfusion system, pro-inflammatory cytokines showed an overall poor expression; conversely, anti-inflammatory ones were the most expressed. The overall data indicated that the perfusion system promoted myogenic commitment with a lower expression of pro-inflammatory cytokines and overexpression of anti-inflammatory ones.

Conclusions and perspectives

The present work described myogenic commitment of *h*BM-MSCs by co-culture with *h*SkMs in a perfused system. The proposed culture seemed more advantageous than the conventional static one, especially owing to easy cell collection. The described system opens perspectives for further studies on more complex cross-talk mechanisms that may involve multiple cell phenotypes. Indeed, the perfused system will easily allow a multiple cell culture with several cell phenotypes to better investigate their specific cross-talk and how they participate to activate molecular signals or cytokines that can exert a fine regulation for muscle regeneration and healing. As an example, the proposed *in vitro* model can be improved with Peripheral Blood Mononuclear Cells (PBMCs) to better understand the role of those cells in myogenic events, alternatively, the perfusion may allow the circulation of biomimetic vesicles fabricated for the targeted delivery of specific signals, in both physiological and pathological simulated conditions.

A deep understanding of the whole biology involved behind stem cell differentiation is still a challenge, and the described model may open perspectives for a comprehensive exploration of stem cell behaviour along with myogenic commitment or for studying a more complex cross-talk between stem cell and myoblast phenotype in health and disease.

Disclosure statement

The authors declare that there is no conflict of interest regarding the publication of this paper. The funders had no role in the design of the study, in the collection, analyses, or interpretation of data, in the writing of the manuscript, or in the decision to publish the results.

Funding

The authors gratefully acknowledge financial support from Athena Srl 139, Viale Europa – 50126 Firenze (IT) under the Research Contract entitled "The design and implementation of a 3D bioengineered model for study on skeletal muscle regeneration and inflammation processes. The year 2020–2021. Principal Investigators: Prof. Nicola Maffulli and Giovanna Della Porta. PS is the recipient of a PhD grant Cycle XXXV in Translational Medicine at Dept. of Medicine, Surgery and Dentistry, the University of Salerno entitled: "Skeletal muscle regeneration modulated by inflammation: an *in vitro* study on a 3D bioengineered system" funded by Athena Srl 139, Viale Europa – 50126 Firenze (IT).

Author contributions

Pasqualina Scala developed the experimental activity and optimised the protocols and methodology; she was responsible for the paper draft preparation and revision; Joseph Lovecchio designed the bioreactor and related operative protocols; Erwin Lamparelli contributed to the experimental activity and qRT-PCR data acquisition; Rossella Vitolo and Valentina Giudice isolated the stem cells and characterised them with formal analysis and validated methodology; Emanuele Giordano supervised the bioreactor protocols; Carmine Selleri provided the methodology for hBM-MSCs cultivation; Laura Rehak provided contribution in supervision and paper writing; Nicola Maffulli helped in the interpretation of the data, reviewed the manuscript and was responsible for funding acquisition; Giovanna Della Porta was responsible for experimental data design, production, curation and supervision, paper writing and editing, funding acquisition and research project administration.

ORCID

C. Selleri http://orcid.org/0000-0002-5861-8984
N. Maffulli http://orcid.org/0000-0002-5327-3702
G. Della Porta http://orcid.org/0000-0002-1426-0159

Data availability statement

All data achieved and described in the present work are available at the following link: https://drive.google.com/drive/folders/1Z-Iufq9eekpTHCwvWFNtXoGrJ4o6AXaW?usp=sharing.

References

[1] Laumonier T, Menetrey J. Muscle injuries and strategies for improving their repair. J Exp Orthop. 2016;3(1):15.
[2] Fernandes TL, Pedrinelli A, Hernandez AJ. Muscle injury – physiopathology, diagnosis, treatment and clinical presentation. Rev Bras Ortop. 2011;46(3):247–255.
[3] Longo UG, Loppini M, Berton A, et al. Tissue engineered strategies for skeletal muscle injury. Stem Cells Int. 2012;2012:1–9.
[4] Qazi TH, Duda GN, Ort MJ, et al. Cell therapy to improve regeneration of skeletal muscle injuries. J Cachexia Sarcopenia Muscle. 2019;10(3):501–516.
[5] Trucillo E, Bisceglia B, Valdrè G, et al. Growth factor sustained delivery from poly-lactic-co-glycolic acid microcarriers and its mass transfer modeling by finite element in a dynamic and static three-dimensional environment bioengineered with stem cells. Biotechnol Bioeng. 2019;116(7):1777–1794.
[6] Ciardulli MC, Marino L, Lamparelli EP, et al. Dose-response tendon-specific markers induction by growth differentiation factor-5 in human bone marrow and umbilical cord mesenchymal stem cells. IJMS. 2020;21(16):5905.
[7] Govoni M, Berardi AC, Muscari C, et al. An engineered multiphase three-dimensional microenvironment to ensure the controlled delivery of cyclic strain and human growth differentiation factor 5 for the tenogenic commitment of human bone marrow mesenchymal stem cells. Tissue Eng Part A. 2017;23(15–16):811–822.
[8] Ciardulli MC, Marino L, Lovecchio J, et al. Tendon and cytokine marker expression by human bone marrow mesenchymal stem cells in a hyaluronate/Poly-Lactic-Co-Glycolic acid (PLGA)/fibrin Three-Dimensional (3D) scaffold. Cells. 2020;9(5):1268.
[9] Witt R, Weigand A, Boos AM, et al. Mesenchymal stem cells and myoblast differentiation under HGF and IGF-1 stimulation for 3D skeletal muscle tissue engineering. BMC Cell Biol. 2017;18(1):15.
[10] Beier JP, Bitto FF, Lange C, et al. Myogenic differentiation of mesenchymal stem cells co-cultured with primary myoblasts. Cell Biol Int. 2011;35(4):397–406.
[11] Ansari S, Chen C, Xu X, et al. Muscle tissue engineering using gingival mesenchymal stem cells encapsulated in alginate hydrogels containing multiple growth factors. Ann Biomed Eng. 2016;44(6):1908–1920.
[12] Gunetti M, Tomasi S, Giammò A, et al. Myogenic potential of whole bone marrow mesenchymal stem cells in vitro and in vivo for usage in urinary incontinence. PLoS One. 2012;7(9):e45538.
[13] Sisson TH, Nguyen M-H, Yu B, et al. Urokinase-type plasminogen activator increases hepatocyte growth factor activity required for skeletal muscle regeneration. Blood. 2009;114(24):5052–5061.
[14] Miller KJ, Thaloor D, Matteson S, et al. Hepatocyte growth factor affects satellite cell activation and differentiation in regenerating skeletal muscle. Am J Physiol Cell Physiol. 2000;278(1):C174–C181.
[15] Tonkin J, Temmerman L, Sampson RD, et al. Monocyte/macrophage-derived IGF-1 orchestrates murine skeletal muscle regeneration and modulates autocrine polarization. Mol Ther. 2015;23(7):1189–1200.
[16] Kästner S, Elias MC, Rivera AJ, et al. Gene expression patterns of the fibroblast growth factors and their receptors during myogenesis of rat satellite cells. J Histochem Cytochem. 2000;48(8):1079–1096.
[17] Conte C, Ainaoui N, Delluc-Clavières A, et al. Fibroblast growth factor 1 induced during myogenesis by a transcription-translation coupling mechanism. Nucleic Acids Res. 2009;37(16):5267–5278.
[18] Scala P, Rehak L, Giudice V, et al. Stem cell and macrophage roles in skeletal muscle regenerative medicine. IJMS. 2021;22(19):10867.
[19] Glennie S, Soeiro I, Dyson PJ, et al. Bone marrow mesenchymal stem cells induce division arrest anergy of activated T cells. Blood. 2005;105(7):2821–2827.
[20] Ribeiro A, Laranjeira P, Mendes S, et al. Mesenchymal stem cells from umbilical cord matrix, adipose tissue and bone marrow exhibit different capability to suppress peripheral blood B, natural killer and T cells. Stem Cell Res. Ther. 2013;4:125.
[21] Bach M, Schimmelpfennig C, Stolzing A. Influence of murine mesenchymal stem cells on proliferation, phenotype, vitality, and cytotoxicity of murine Cytokine-Induced killer cells in coculture. PLoS One. 2014;9(2):e88115.
[22] Kudlik G, Hegyi B, Czibula Á, et al. Mesenchymal stem cells promote macrophage polarization toward M2b-like cells. Exp Cell Res. 2016;348(1):36–45.
[23] El-Sayed M, El-Feky MA, El-Amir MI, et al. Immunomodulatory effect of mesenchymal stem cells: cell origin and cell quality variations. Mol Biol Rep. 2019;46(1):1157–1165.
[24] Corcione A, Benvenuto F, Ferretti E, et al. Human mesenchymal stem cells modulate B-cell functions. Blood. 2006;107(1):367–372.
[25] Ramasamy R, Fazekasova H, W Lam EF, et al. Mesenchymal stem cells inhibit dendritic cell differentiation and function by preventing entry into the cell cycle. Transplantation. 2007;83(1):71–76.
[26] Carrier RL, Rupnick M, Langer R, et al. Perfusion improves tissue architecture of engineered cardiac muscle. Tissue Eng. 2002;8(2):175–188.
[27] Lovecchio J, Gargiulo P, Vargas Luna JL, et al. A standalone bioreactor system to deliver compressive load under perfusion flow to hBMSC-seeded 3D chitosan-graphene templates. Sci Rep. 2019;9(1):16854.
[28] Kim J, Ma T. Perfusion regulation of hMSC microenvironment and osteogenic differentiation in 3D scaffold. Biotechnol Bioeng. 2012;109(1):252–261.

[29] Lamparelli EP, Lovecchio J, Ciardulli MC, et al. Chondrogenic commitment of human bone marrow mesenchymal stem cells in a perfused collagen hydrogel functionalized with hTGF-β1-Releasing PLGA microcarrier. Pharmaceutics. 2021;13(3):399.

[30] Lovecchio J, Pannella M, Giardino L, et al. A dynamic culture platform enhances the efficiency of the 3D HUVEC-based tube formation assay. Biotechnol Bioeng. 2020;117(3):789–797.

[31] Pasini A, Lovecchio J, Cortesi M, Liverani C, Spadazzi C, Mercatali L, Ibrahim T, Giordano E. Perfusion Flow Enhances Viability and Migratory Phenotype in 3D-Cultured Breast Cancer Cells. Ann Biomed. Eng. 2021 Sep;49(9):2103–2113. doi: 10.1007/s10439-021-02727-w. Epub 2021 Feb 4. P MID: 33543395; P MCID: P MC8455496.

[32] Han TTY, Walker JT, Grant A, et al. Preconditioning human adipose-derived stromal cells on decellularized adipose tissue scaffolds within a perfusion bioreactor modulates cell phenotype and promotes a pro-regenerative host response. Front Bioeng Biotechnol. 2021;9:642465.

[33] Ciardulli MC, Lovecchio J, Scala P, et al. 3D biomimetic scaffold for growth factor controlled delivery: an in-vitro study of tenogenic events on Wharton's jelly mesenchymal stem cells. Pharmaceutics. 2021;13(9):1448.

[34] Agrawal G, Aung A, Varghese S. Skeletal muscle-on-a-chip: an in vitro model to evaluate tissue formation and injury. Lab Chip. 2017;17(20):3447–3461.

[35] Phan DTT, Wang X, Craver BM, et al. A vascularized and perfused organ-on-a-chip platform for large-scale drug screening applications. Lab Chip. 2017;17(3):511–520.

[36] Viswanathan S, Shi Y, Galipeau J, et al. Mesenchymal stem versus stromal cells: international society for cell & gene therapy (ISCT®) mesenchymal stromal cell committee position statement on nomenclature. Cytotherapy. 2019;21(10):1019–1024.

[37] Satyavrata Samavedi, Lauren K. Poindexter, Mark Van Dyke and Aaron S. Goldstein. Chapter 7 - Synthetic Biomaterials for Regenerative Medicine Applications, In Regenerative Medicine Applications in Organ Transplantation, edition edited by Giuseppe Orlando, Jan Lerut, Shay Soker and Robert J. Stratta, Academic Press, Boston, 2014. Pages. 81–99, ISBN 9780123985231. https://doi.org/10.1016/B978-0-12-398523-1.00007-0

[38] Pasini A, Lovecchio J, Ferretti G, et al. Medium perfusion flow improves osteogenic commitment of human stromal cells. Stem Cells Int. 2019;(2019):1–10.

[39] Hellemans J, Mortier G, De Paepe A, et al. qBase relative quantification framework and software for management and automated analysis of real-time quantitative PCR data. Genome Biol. 2007;8(2):R19.

[40] Suchorska WM, Lach MS, Richter M, et al. Bioimaging: an useful tool to monitor differentiation of human embryonic stem cells into chondrocytes. Ann Biomed Eng. 2016;44(5):1845–1859.

[41] de Winter J.C.F. (2013) "Using the Student's t-test with extremely small sample sizes," Practical Assessment, Research, and Evaluation: Vol. 18 , Article 10. DOI: https://doi.org/10.7275/e4r6-dj05

[42] Dominici M, Le Blanc K, Mueller I, et al. Minimal criteria for defining multipotent mesenchymal stromal cells. The international society for cellular therapy position statement. Cytotherapy. 2006;8(4):315–317.

[43] Bentzinger CF, Wang YX, Rudnicki MA. Building muscle: molecular regulation of myogenesis. Cold Spring Harb Perspect. Biol. 2012;4(2):a008342–a008342.

[44] Plotnikov EY, Khryapenkova TG, Vasileva AK, et al. Cell-to-cell cross-talk between mesenchymal stem cells and cardiomyocytes in co-culture. J Cell Mol Med. 2008;12(5A):1622–1631.

[45] Liu X, Chen W, Zhang C, et al. Co-seeding human endothelial cells with human-induced pluripotent stem cell-derived mesenchymal stem cells on calcium phosphate scaffold enhances osteogenesis and vascularization in rats. Tissue Eng Part A. 2017;23(11–12):546–555.

[46] Asfour HA, Allouh MZ, Said RS. Myogenic regulatory factors: the orchestrators of myogenesis after 30 years of discovery. Exp Biol Med. 2018;243(2):118–128.

[47] Shang YC, Zhang C, Wang SH, et al. Activated beta-catenin induces myogenesis and inhibits adipogenesis in BM-derived mesenchymal stromal cells. Cytotherapy. 2007;9(7):667–681.

[48] Kozlowska U, Krawczenko A, Futoma K, et al. Similarities and differences between mesenchymal stem/progenitor cells derived from various human tissues. World J Stem Cells. 2019;11(6):347–374.

[49] Chen S-E, Jin B, Li Y-P. TNF-alpha regulates myogenesis and muscle regeneration by activating p38 MAPK. Am J Physiol Cell Physiol. 2007;292(5):C1660–C1671.

[50] Li Y-P, Schwartz RJ. TNF-alpha regulates early differentiation of C2C12 myoblasts in an autocrine fashion. Faseb J. 2001;15(8):1413–1415.

[51] Li Y-P. TNF-alpha is a mitogen in skeletal muscle. Am J Physiol Cell Physiol. 2003;285(2):C370–C376.

[52] Zhao Q, Yang ST, Wang JJ, et al. TNF alpha inhibits myogenic differentiation of C2C12 cells through NF-κB activation and impairment of IGF-1 signaling pathway. Biochem Biophys Res Commun. 2015;458(4):790–795.

[53] Grabiec K, Tokarska J, Milewska M, et al. Interleukin-1beta stimulates early myogenesis of mouse C2C12 myoblasts: the impact on myogenic regulatory factors, extracellular matrix components, IGF binding proteins and protein kinases. Pol J Vet Sci. 2013;16(2):255–264.

[54] Li W, Moylan JS, Chambers MA, et al. Interleukin-1 stimulates catabolism in C2C12 myotubes. Am J Physiol Cell Physiol. 2009;297(3):C706–C714.

[55] Deng B, Wehling-Henricks M, Villalta SA, et al. IL-10 triggers changes in macrophage phenotype that promote muscle growth and regeneration. J Immunol. 2012;189(7):3669–3680.

[56] Horsley V, Jansen KM, Mills ST, et al. IL-4 acts as a myoblast recruitment factor during mammalian muscle growth. Cell. 2003;113(4):483–494.

[57] Chang Y-H, Tsai J-N, Chen T-L, et al. Interleukin-4 promotes myogenesis and boosts myocyte insulin efficacy. Mediators Inflamm. 2019;(2019):1–14.